Optimal Location of Unified Power Flow Contrller Considering Power Flow and Transient Stability

***Naseer M. Yasin** ****Dr. Mustafa M. Al-Eedany**
Ass. Prof.

Abstract

Unified Power Flow Controller (UPFC) is a well known device for effectively regulating the active and reactive power flow in a power system. In this paper, the UPFC linearized power flow equations are incorporated into Newton-Raphson algorithm in a MATLAB written program to determine the optimal location of UPFC using Genetic Algorithm, considering control of active and reactive power flow, and the transient stability of a five bus IEEE test systems. A comparison of the results obtained for the base case without UPFC and with it, is made to investigate the effectiveness of the device.

Key words: Load flow analysis, Newton-Raphson, UPFC.

Introduction

Rapid development of power systems especially with the increased use of transmission facilities has necessitated new ways of maximizing power transfer in existing transmission facilities, while at the same time maintaining the same level of stability [1].

Monitoring the stability status of a power system in real time has been recognized as a task of primary importance in preventing blackouts. In case of a disturbance leading to transient instability, fast recognition of the potentially dangerous conditions is very crucial for allowing sufficient time to take emergency control actions. Several attempts to develop an effective real-time transient stability indicator have been reported in the literature [2–4].

The transient stability of power systems is associated with the ability of the generators to remain in synchronism after a severe disturbance [5]. It depends upon the severity of the contingency and the initial operating state of the power systems. Here the term contingency, also called disturbance or fault, indicates an event like the three-phase short circuit in the grid that will cause large changes in the power system [6]. The operating power system will first encounter the hurdle of transient stability before apparatuses thermal limits [7]. When a contingency occures in the electrical network, the power system is likely to lose stability, or may be even worse to trigger large scale blackouts [8].

In order to avoid catastrophic outages, power utilities resort to various planning, protection and control schemes. Preventive control is summoned up when the power system is still in normal status. It encompasses many types of control actions, including generation rescheduling, load curtailment and network switching reactive compensation [9,10]. Those preventive control actions reallocate power system operating state so that it can guarantee satisfactory behavior after a contingency occurred in the grid.

The real time Transient Stability Assessment (TSA) is important to the power system security and efficient operation. Otherwise essential control actions could be delayed, which

in turn could trigger a large scale blackout. Further, real time TSA will avoid any unnecessary control commands to ensure the minimum impact on the grid.

The conventional transient stability measure of a system's robustness to withstand a large disturbance is its corresponding Critical Clearing Time (CCT) which is the maximum time duration for which the disturbance may act without the system losing its capability to recover a steady-state (i.e., stable) operation [11].

In the late 1980s, the Electric Power Research Institute (EPRI) formulated the vision of the Flexible AC Transmission Systems (FACTS) in which various power-electronics based controllers regulate power flow and transmission voltage and mitigate dynamic disturbances. Fast development of power electronic technology has made FACTS promising solution of the future power system. FACTS controllers such as Static Synchronous Compensator (STATCOM), Static VAR Compensator (SVC), Thyristor Controlled Series Compensator (TCSC), Static Synchronous Series Compensator (SSSC) and Unified Power Flow Controller (UPFC) are able to change the network parameters in a fast and effective way in order to achieve better system performance [12-14].

These controllers are used for enhancing dynamic performance of power systems in terms of voltage/angle stability while improving the power transfer capability and voltage profile in steady-state conditions [15-17].

In [18], the modeling of FACTS devices for power flow studies and the role of that modeling in the study of FACTS devices for power flow control are discussed. Three essential generic models of FACTS devices are presented and the combination of those devices into load flow analysis, studies relating to wheeling, and interchange power flow control is explained. The determination of the voltage magnitude and phase angle of the FACTS bus is provided by solving two simultaneous nonlinear equations. These equations are solved with a separate Newton-Raphson approach within each iteration of the large load flow analysis.

In [19], various control methods for damping undesirable inter-area oscillations by power system stabilizers (PSS), SVCs and STATCOMs are discussed. It is observed that the damping introduced by the SVC and STATCOM controllers with only voltage control was lower than that provided by the PSSs and the STATCOM provides better damping than the SVC as this controller is able to transiently exchange active power with the system.

In [20], the issue of UPFC modeling within the context of optimal power flow solutions is addressed. The UPFC model has been presented to control active and reactive power flow at the buses of the sending or receiving end. The UPFC model suitable for optimal power flow solutions is presented for the first time in this study.

Unified Power Flow Controller (UPFC)

The UPFC may be seen to consist of two voltage source converters (VSC) sharing a common capacitor on their DC side and a unified control system. A simplified schematic representation of the UPFC is given in Figure (1), together with its equivalent circuit, in Figure (2) [21]. The UPFC allows simultaneous control of active power flow, reactive power flow, and voltage magnitude at the UPFC terminals. Alternatively, the controller may be set to control one or more of these parameters in any combination or to control none of them [22].

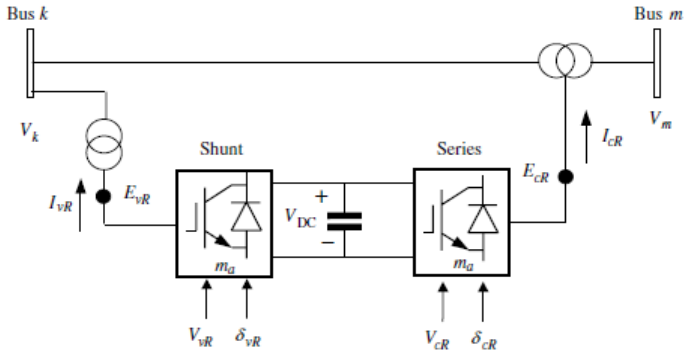

Figure 1: Unified power flow controller (UPFC) system, two back-to-back voltage source converters (VSCs)

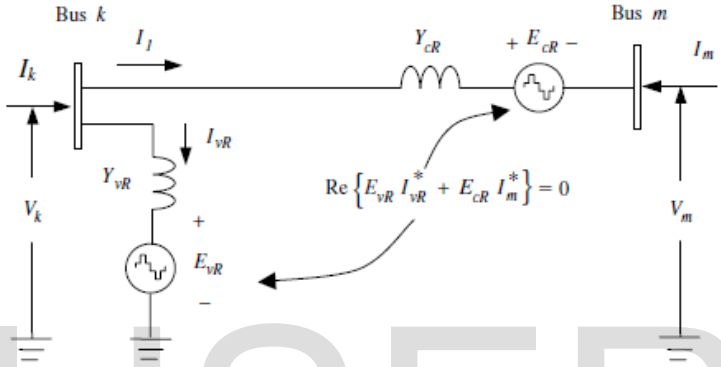

Figure 2: Unified power flow controller (UPFC) system, equivalent circuit based on solid-state voltage sources.

The active power demanded by the series converter is drawn by the shunt converter from the AC network and supplied to bus m through the DC link. The output voltage of the series converter is added to the nodal voltage, at bus k, to boost the nodal voltage at bus m. The voltage magnitude of the output voltage V_{cR} provides voltage regulation, and the phase angle δ_{cR} determines the mode of power flow control [12].

In addition to providing a supporting role in the active power exchange that takes place between the series converter and the AC system, the shunt converter may also generate or absorb reactive power in order to provide independent voltage magnitude regulation at its point of connection with the AC system.

Modeling of UPFC

The UPFC equivalent circuit shown in Figure (2) consists of a shunt-connected voltage source, a series-connected voltage source, and an active power constraint equation, which links the two voltage sources. The two voltage sources are connected to the AC system through inductive reactances representing the voltage source converter transformers.

Based on the equivalent circuit, the following transfer admittance equation can be written:

$$\begin{bmatrix} I_k \\ I_m \end{bmatrix} = \begin{bmatrix} Y_{cR} + Y_{vR} & -Y_{cR} & -Y_{cR} & -Y_{vR} \\ -Y_{cR} & Y_{cR} & Y_{cR} & 0 \end{bmatrix} \begin{bmatrix} V_k \\ V_m \\ E_{cR} \\ E_{vR} \end{bmatrix} \quad (1)$$

Expressions for the two voltage sources and constraint equation would be:

$$E_{vR} = V_{vR}(cos\delta_{vR} + jsin\delta_{vR}) \quad (2)$$
$$E_{cR} = V_{cR}(cos\delta_{cR} + jsin\delta_{cR}) \quad (3)$$
$$Re(E_{vR}I_{vR}^{*} + E_{cR}I_{m}^{*}) = 0 \quad (4)$$

The phase angle of the series-injected voltage determines the mode of power flow control. If δ_{cR} is in phase with the nodal voltage angle δ_k, the UPFC regulates the terminal voltage. If δ_{cR} is in quadature with respect to δ_k, it controls active power flow. If δ_{cR} is in quadrature with the line current angle then it controls active power flow, acting as a variable series compensator. At any other value of δ_{cR}, the UPFC operates as a combination of voltage regulator, variable series compensator. The magnitude of the series-injected voltage determines the amount of power flow to be controlled. Based on the equivalent circuit shown in Figure (2) and Equations (2) and (3), the active and reactive power equations are [23]:

$$P_k = V_k^2 G_{kk} + V_k V_m[G_{km}\cos(\delta_k - \delta_m) + B_{km}\sin(\delta_k - \delta_m)] + V_k V_{cR}[G_{km}\cos(\delta_k - \delta_{cR}) + B_{km}\sin(\delta_k - \delta_{cR})] + V_k V_{vR}[G_{vR}\cos(\delta_k - \delta_{vR}) + B_{vR}\sin(\delta_k - \delta_{vR})] \quad (5)$$

$$Q_k = -V_k^2 B_{kk} + V_k V_m[G_{km}\sin(\delta_k - \delta_m) - B_{km}\cos(\delta_k - \delta_m)] + V_k V_{cR}[G_{km}\sin(\delta_k - \delta_{cR}) - B_{km}\cos(\delta_k - \delta_{cR})] + V_k V_{vR}[G_{vR}\sin(\delta_k - \delta_{vR}) - B_{vR}\cos(\delta_k - \delta_{vR})] \quad (6)$$

$$P_{cR} = V_{cR}^2 G_{mm} + V_{cR} V_k[G_{km}cos(\delta_{cR} - \delta_k) + B_{km}\sin(\delta_{cR} - \delta_k)] + V_{cR} V_m[G_{mm}cos(\delta_{cR} - \delta_m) + B_{mm}\sin(\delta_{cR} - \delta_m)] \quad (9)$$

$$Q_{cR} = -V_{cR}^2 B_{mm} + V_{cR} V_k[G_{km}sin(\delta_{cR} - \delta_k) - B_{km}\cos(\delta_{cR} - \delta_k)] + V_{cR} V_m[G_{mm}sin(\delta_{cR} - \delta_m) - B_{mm}\cos(\delta_{cR} - \delta_m)] \quad (10)$$

$$P_{vR} = -V_{vR}^2 G_{vR} + V_{vR} V_k[G_{vR}cos(\delta_{vR} - \delta_k) + B_{vR}\sin(\delta_{vR} - \delta_k)] \quad (11)$$

$$Q_{vR} = V_{vR}^2 B_{vR} + V_{vR} V_k[G_{vR}sin(\delta_{vR} - \delta_k) - B_{vR}\cos(\delta_{vR} - \delta_k)] \quad (12)$$

Assuming loss-less converter, the active power supplied to the shunt converter, P_{vR}, equals the active power demanded by the series converter, P_{cR}, that is:

$$P_{vR} + P_{cR} = 0 \quad (13)$$

Furthermore, if the coupling transformers are assumed to contain no resistance then the active power at bus k matches the active power at bus m, therefore

$$P_k + P_m = 0 \quad (14)$$

The UPFC power equations, in linearized form, are combined with those of the AC network. For the case when the UPFC controls the voltage magnitude at the shunt converter terminal (bus k), active power flow from bus m to bus k, and reactive power injected at bus m. The linearized system equations are as follows:

$$\begin{bmatrix} \Delta P_k \\ \Delta P_m \\ \Delta Q_k \\ \Delta Q_m \\ \Delta P_{mk} \\ \Delta Q_{mk} \\ \Delta P_{bb} \end{bmatrix} = \begin{bmatrix} \frac{\partial P_k}{\partial \delta_k} & \frac{\partial P_k}{\partial \delta_m} & \frac{\partial P_k}{\partial V_{vR}} & \frac{\partial P_k}{\partial V_m} & \frac{\partial P_k}{\partial \delta_{cR}} & \frac{\partial P_k}{\partial V_{cR}} & \frac{\partial P_k}{\partial \delta_{vR}} \\ \frac{\partial P_m}{\partial \delta_k} & \frac{\partial P_m}{\partial \delta_m} & 0 & \frac{\partial P_m}{\partial V_m} & \frac{\partial P_m}{\partial \delta_{cR}} & \frac{\partial P_m}{\partial V_{cR}} & 0 \\ \frac{\partial Q_k}{\partial \delta_k} & \frac{\partial Q_k}{\partial \delta_m} & \frac{\partial Q_k}{\partial V_{vR}} & \frac{\partial Q_k}{\partial V_m} & \frac{\partial Q_k}{\partial \delta_{cR}} & \frac{\partial Q_k}{\partial V_{cR}} & \frac{\partial Q_k}{\partial \delta_{vR}} \\ \frac{\partial Q_m}{\partial \delta_k} & \frac{\partial Q_m}{\partial \delta_m} & 0 & \frac{\partial Q_m}{\partial V_m} & \frac{\partial Q_m}{\partial \delta_{cR}} & \frac{\partial Q_m}{\partial V_{cR}} & 0 \\ \frac{\partial P_{mk}}{\partial \delta_k} & \frac{\partial P_{mk}}{\partial \delta_m} & 0 & \frac{\partial P_{mk}}{\partial V_m} & \frac{\partial P_{mk}}{\partial \delta_{cR}} & \frac{\partial P_{mk}}{\partial V_{cR}} & 0 \\ \frac{\partial Q_{mk}}{\partial \delta_k} & \frac{\partial Q_{mk}}{\partial \delta_m} & 0 & \frac{\partial Q_{mk}}{\partial V_m} & \frac{\partial Q_{mk}}{\partial \delta_{cR}} & \frac{\partial Q_{mk}}{\partial V_{cR}} & 0 \\ \frac{\partial P_{bb}}{\partial \delta_k} & \frac{\partial P_{bb}}{\partial \delta_m} & \frac{\partial P_{bb}}{\partial V_{vR}} & \frac{\partial P_{bb}}{\partial V_m} & \frac{\partial P_{bb}}{\partial \delta_{cR}} & \frac{\partial P_{bb}}{\partial V_{cR}} & \frac{\partial P_{bb}}{\partial \delta_{vR}} \end{bmatrix} \begin{bmatrix} \Delta \delta_k \\ \Delta \delta_m \\ \Delta V_{vR} \\ \Delta V_m \\ \Delta \delta_{cR} \\ \Delta V_{cR} \\ \Delta \delta_{vR} \end{bmatrix} \quad (15)$$

Where ΔP_{bb} is the power mismatch given by Equation (13).

Power Formulae for Transmission Lines [24]

Let the sending end voltage $V_s = |V_s|\angle\delta$, and the receiving end voltage $V_r = |V_r|\angle 0$.

Using the generalized line constants $D = A = |A|\angle\alpha$ and $B = |B|\angle\beta$. The complex power per phase at the receiving end is

$$S_r = \frac{|V_s||V_r|}{|B|}\angle(\beta - \delta) - \frac{|A||V_r|^2}{|B|}\angle(\beta - \alpha) \quad (16)$$

$$P_r = \frac{|V_s||V_r|}{|B|}cos(\beta - \delta) - \frac{|A||V_r|^2}{|B|}cos(\beta - \alpha) \quad (17)$$

The received power is maximum when $\beta = \delta$

$$P_{rmax} = \frac{|V_s||V_r|}{|B|} - \frac{|A||V_r|^2}{|B|}cos(\beta - \alpha) \quad (18)$$

Overview of Genetic Algorithm [25]

Genetic Algorithm (GA) is an optimization algorithm which is based on natural evolution. In each generation of GA, a new set of chromosomes with improved fitness is produced using genetic operators (i.e. selection, crossover and mutation).

Selection Operator: Gives preference to better individuals, allowing them to pass on their genes to the next generation. The goodness of each individual depends on its fitness. Fitness may be determined by an objective function or by a subjective judgement.

Crossover Operator: Prime distinguished factor of GA from other optimization techniques. Two individuals are chosen from the population using the selection operator .A crossover site along the bit strings is randomly chosen. The values of the two strings are exchanged up to this point. The two new offspring created from this mating are put into the next generation.

Mutation Operator: With some low probability, a portion of the new individuals will have some of their bits flipped. Its purpose is to maintain diversity within the population and inhibit premature convergence.

GA Based Optimal Location

GA is interduced for the determination of optimal location of FACTS devices implemented in any branch throughout the inter-connected power system. The search is conducted so as to find the point at which the active received power P_r is maximum, that is the objective function is P_{rmax} as given by Equation (18). The branch distance between two buses is divided into two sections, one is termed S, the distance from the sending end to the FACTS device, while the other is 1-S, as in Figure (3). The FACTS device point of connection is then changed randomly on the branch to find the best distance from the sending end for the FACTS to be placed, that is to find S.

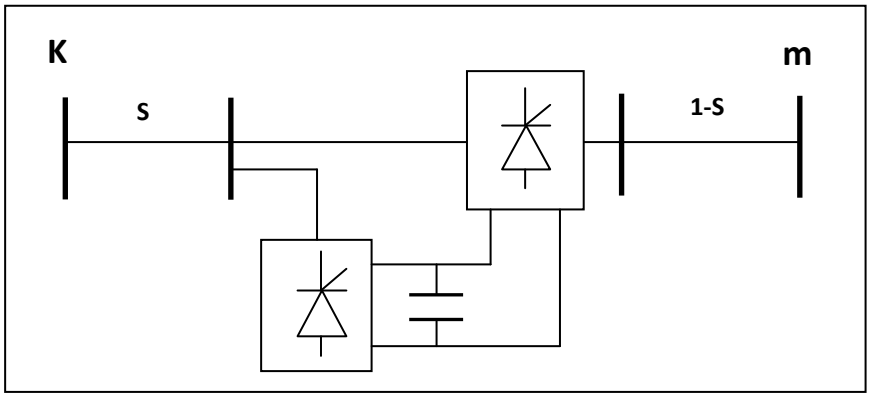

Figure 3: Equivalent Circuit of UPFC Connected Between Two Virtual Buses.

Simulation and Results

The IEEE 5-bus system in Figure (4), the data of which can be found in [23], is used to test the effectiveness of connecting the UPFC device between bus3 and bus4. Using Newton-Raphson method, the load flow and power flow results of the system without the UPFC connected are shown in Table (1&2).

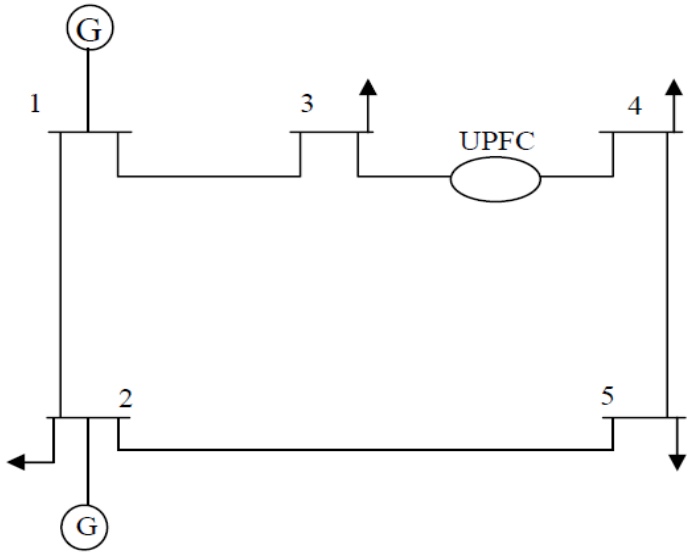

Figure 4: IEEE 5-bus power system with UPFC

Table 1: Load flow results of 5-bus test system without UPFC

Power Flow Solution by Newton-Raphson Method						
Maximum Power Mismatch = 2.84495e-015						
No. of Iterations = 5						
Bus	Voltage	Angle	------Load------		---Generation--	
No.	Mag.	Degree	MW	MVAR	MW	MVAR
1	1.060	0.000	0.000	0.000	131.122	90.816
2	1.000	-2.061	20.000	10.000	40.000	-61.593
3	0.987	-4.637	45.000	15.000	0.000	0.000
4	0.984	-4.957	40.000	5.000	0.000	0.000
5	0.972	-5.765	60.000	10.000	0.000	0.000
Total			165.000	40.000	171.122	29.223

Table 2: Line flow results of 5-bus test system without UPFC

Line Flow and Losses						
--Line--		Power at bus & line flow			--Line loss--	
From	To	MW	MVAR	MVA	MW	MVAR
1		131.122	90.816	159.501		
	2	89.331	73.995	115.997	2.486	1.087
	3	41.791	16.820	45.049	1.518	-0.692
2		20.000	-71.593	74.334		
	1	-86.846	-72.908	113.392	2.486	1.087
	3	24.473	-2.518	24.602	0.360	-2.871
	4	27.713	-1.724	27.767	0.461	-2.554
	5	54.660	5.558	54.942	1.215	0.729
3		-45.000	-15.000	47.434		
	1	-40.273	-17.513	43.916	1.518	-0.692
	2	-24.113	-0.352	24.116	0.360	-2.871
	4	**19.386**	**2.865**	19.597	0.040	-1.823
4		-40.000	-5.000	40.311		
	2	-27.252	-0.831	27.265	0.461	-2.554
	3	-19.346	-4.688	19.906	0.040	-1.823
	5	6.598	0.518	6.619	0.043	-4.652
5		-60.000	-10.000	60.828		
	2	-53.445	-4.829	53.663	1.215	0.729
	4	-6.555	-5.171	8.349	0.043	-4.652
Total loss					6.122	-10.777

For the system without the UPFC. A three phase fault is created at transmission line 1-3 near bus1, the protecting relays isolate the fault by removing this faulty line. A plot of the power angle difference between the two generators at bus1 (slack bus) and bus2 (voltage controlled bus) which means (δ2-δ1) is shown in Figure (5). The swing curve shows that the power system is stable for CCT=0.456sec. and loses stability for clearing time of Tc=0.457sec.

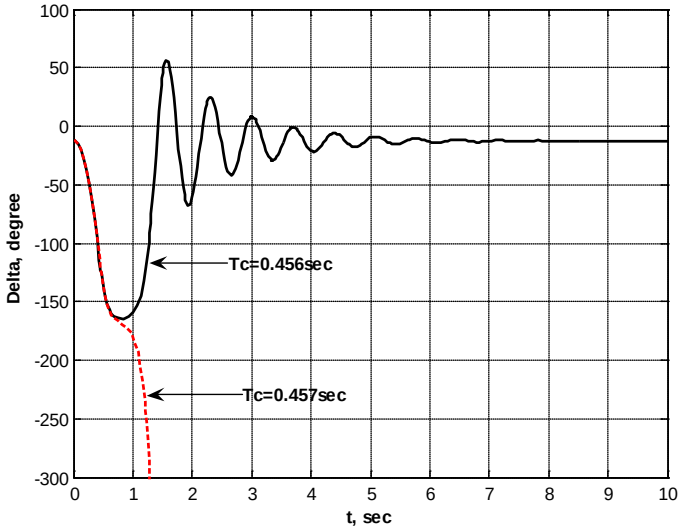

Figure 5: Power angle Difference for 5-bus test system, fault at T.L. 1-3

The UPFC is used to maintain active and reactive powers leaving the UPFC towards bus4, at 40 MW and 2MVAR, respectively. Moreover, the UPFC shunt converter is set to regulate the nodal voltage magnitude of bus3 at 1pu. The starting values of the voltage sources are taken to be $V_{cR} = 0.04pu$, $\delta_{cR} = -87°$, $V_{vR} = 1.0pu$, and $\delta_{vR} = 0°$. The source impedances have values of $X_{cR} = X_{vR} = 0.1pu$. Convergence is obtained in seven iterations to a power mismatch tolerance of 1e-13. The UPFC upheld its target values. Load flow results and power flow are shown in Tables (3&4) respectively.

Table 3: Load flow results of 5-bus test system with UPFC

Power flow Solution by Newton-Raphson Method						
Maximum Power Mismatch = 2.71921e-013						
No. of Iterations = 7						
B	Voltage	Angle	------Load------		---Generation---	
N	Mag.	Degree	MW	MVAR	MW	MVAR
1	1.060	0.000	0.000	0.000	131.484	85.767
2	1.000	-1.769	20.000	10.000	40.000	-75.487
3	**1.000**	-6.016	45.000	15.000	0.000	0.000
4	0.992	-3.191	40.000	5.000	0.000	0.000
5	0.975	-4.974	60.000	10.000	0.000	0.000
6	0.997	-2.512	0.000	0.000	0.000	0.000
Total			165.000	40.000	171.484	10.280

Table 4: Line flow results of 5-bus test system with UPFC

Line Flow and Losses						
--Line-- Power at bus & line flow					--Line loss--	
From	To	MW	MVAR	MVA	MW	MVAR
1		131.484	85.767	156.984		
	2	81.143	76.424	111.467	2.305	0.545
	3	50.341	9.343	51.200	1.909	0.419
2		20.000	-85.487	87.796		
	1	-78.838	-75.879	109.421	2.305	0.545
	3	37.484	-12.969	39.664	0.915	-1.254
	4	13.739	-1.780	13.854	0.113	-3.627
	5	47.614	5.140	47.891	0.924	-0.151
3		-45.000	-15.000	47.434		
	1	-48.431	-8.924	49.246	1.909	0.419
	2	-36.569	11.715	38.399	0.915	-1.254
	6	-60.902	5.352	61.137	0.000	3.738
4		-40.000	-5.000	40.311		
	2	-13.626	-1.847	13.750	0.113	-3.627
	6	-39.838	-3.490	39.991	0.162	-1.490
	5	13.464	0.337	13.468	0.154	-4.371
5		-60.000	-10.000	60.828		
	2	-46.690	-5.291	46.989	0.924	-0.151
	4	-13.310	-4.709	14.118	0.154	-4.371
6		0.000	0.000	0.000		
	3	60.902	-1.614	60.924	0.000	3.738
	4	**40.000**	**2.000**	40.050	0.162	-1.490
Total loss					6.484	-6.191

To test the modified power system for the stability enhancement, the same fault that was created near bus1 at transmission line 1-3 is simulated. The power angle curve plotted in Figure (6) shows that the system is considered stable for CCT=0.468sec. This means that the power system has acquired an increase of 2.63% as compared with the base case.

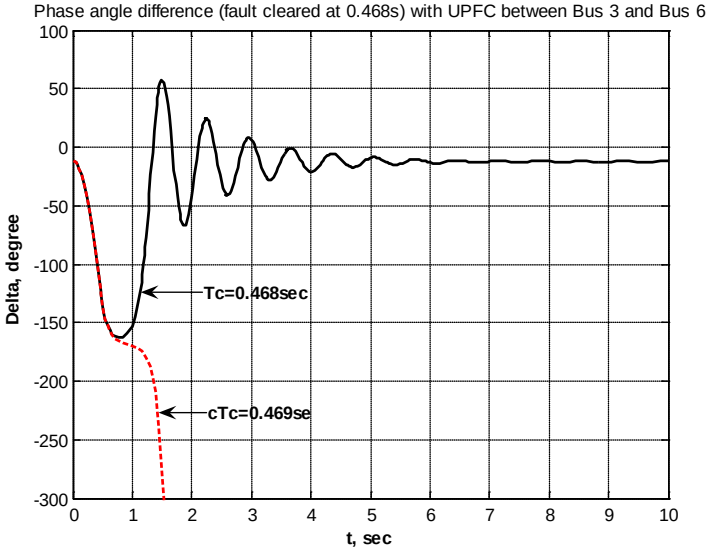

Figure 6: Power angle curve for 5-bus test system, fault at T.L. 1-3

Results of GA with UPFC

The compensating reactances X_{CR}, X_{VR} are combined in the transfer matrix to determine the new line parameters, as shown below:

$$\begin{bmatrix} A & B \\ C & D \end{bmatrix} = \begin{bmatrix} 1+\frac{S^2ZY}{2} & SZ \\ SY\left(1+\frac{S^2ZY}{4}\right) & 1+\frac{S^2ZY}{2} \end{bmatrix} \begin{bmatrix} 1 & JX_{CR} \\ JB_{VR} & 1 \end{bmatrix} \begin{bmatrix} 1+\frac{(1-S)^2ZY}{2} & (1-S)Z \\ (1-S)Y\left(1+\frac{(1-S)^2ZY}{4}\right) & 1+\frac{(1-S)^2ZY}{2} \end{bmatrix} \quad (19)$$

$$A = \left(\left(1+\frac{S^2ZY}{2}\right)+SZJB_{VR}\right)\left(1+\frac{(1-S)^2ZY}{2}\right)+\left(\left(1+\frac{S^2ZY}{2}\right)JX_{CR}+SZ\right)\left((1-s)Y(1+\frac{(1-S)^2ZY}{4}\right) \quad (20)$$

$$B = \left(\left(1+\frac{S^2ZY}{2}\right)+SZJB_{VR}\right)\left((1-S)Z\right)+\left(\left(1+\frac{S^2ZY}{2}\right)JX_{CR}+SZ\right)\left(1+\frac{(1-S)^2ZY}{2}\right) \quad (21)$$

Where z is the impedance of the line between bus k and m, Y is the susceptance.

To determine the maximum power received P_{rmax} using the above line parameters, the following results are obtained for installing the UPFC in the branch between bus3 and bus4 for the IEEE 5-bus test power system, in Table (5),and in Figure (7).

Table 5: GA Results for UPFC between Bus3 and Bus4

* Binary Genetic Algorithm
* Each parameter is represented by 16 bits
* Populatin size=12 Mutation rate=0.1
* #par=1 #generations=10
* Best Location =0.10656=S
* Best cost=703.606

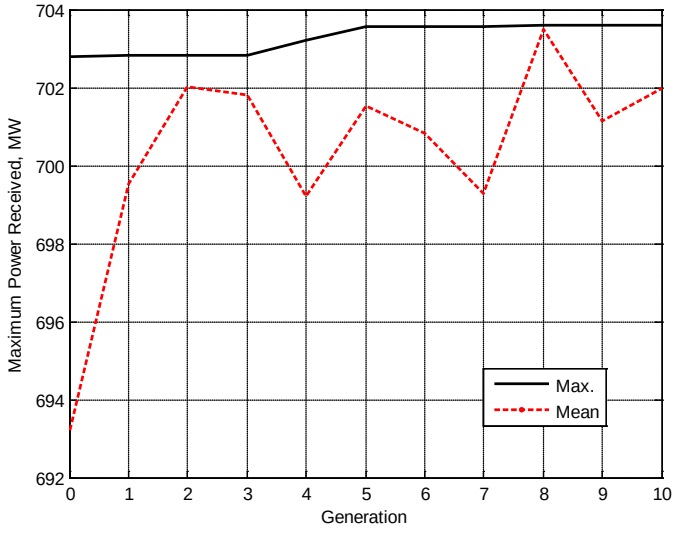

Figure 7: Maximum power received for UPFC between Bus3 and Bus4.

The UPFC is now positioned at $S = 0.1$ between bus3 and bus4, and the same fault created near bus1 at transmission line 1-3 for the base case, is now simulated, and the power angle curve is plotted in Figure (8). It can be seen that the power system is stable for CCT=0.468sec, which is the same value as that obtained when the UPFC was connected at bus3.

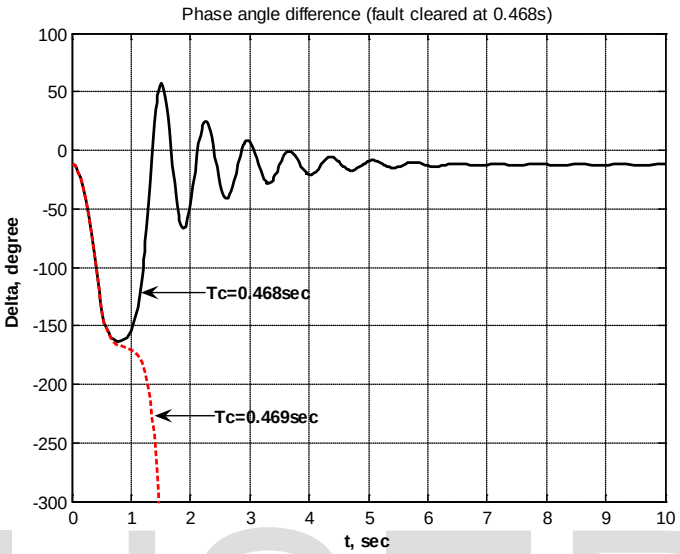

Figure 8: Power angle curve for 5-bus test system, fault at T.L. 1-3

Therefore connecting the UPFC at 0.1 of the distance between bus3 and bus4 has the same ability of enhancing the power flow. More over, it ensures maximum power received at bus4.

Conclusions

In this paper the model for power flow and transient stability for an IEEE five bus test systems with the UPFC included was developed and the results for specifying the active power flow in a certain branch of the power system were verified, it was found that the active power in branch (3-4) could be increased by nearly 20.6MW for the IEEE-5 bus test system. The transient stability was also tested and the results show that the stability margin was increased with the inclusion of the UPFC device for the IEEE-5 bus by 2.63%.

References

[1]. M. O. Hassen, S.J.Cheng and Z. A. Zakaria "Steady State Modelling of SVC and TCSC for power Flow Analysis" *Proc.* of the *Inter. Multiconferance* of Engineering and Computer Scientists Vol.2, 2009.

[2]. F. F. Song, T. S. Bi, and Q. X. Yang, “Study on Wide Area Measurement System Based Transient Stability Control for Power Systems,” in *Proc. IPEC Power Engineering Conf.*, Vol. 2, 2005, pp. 757–760.

[3]. A. G. Phadke, "Synchronized Phasor Measurements in Power Systems," *IEEE Computer Appl. Power*, Vol. 6, No. 2, Apr. 1993, pp. 10–15.

[4]. H. Dongchen and V. Venkatasubramanian, "New Wide-Area Algorithms for Detection and Mitigation of Angle Instability Using Synchrophasors," in *Proc*. Power Eng. Soc. General Meeting, June 2007, pp. 1–8.

[5]. P. Kundur, 1. Paserba and V. Ajjarapu , " Definition and Classification of Power System Stability IEEE/CIGRE Joint Task Force on Stability Terms and Definitions," IEEE *Trans*. on *Power Systems*, Vol**.** 19, Aug. 2004, pp. 1387-1401.

[6]. M. Pavella, D. Ernst and D. Ruiz-Vega, "Transient Stability of Power Systems," Kluwer Academic Publishers, 2000,pp.6

[7]. A. Olwegard, K. Walve, G. Waglund, H. Frank and S. Toresng, "Improvement of Transimission Capacity by Thyristor Controlled Reactive Power," IEEE *Trans*. on Power Apparatus and Systems, Vol. 100, No. 8, 1981, pp. 3930-3939.

[8]. P. Poubeik, P. S. Kundur, and C. W. Taylor, "The Anatomy of a Power Grid Blackout - Root Causes and Dynamics of Recent Major Blackouts ," IEEE *Power & Energy Magazine*, Vol. 4, Sep/Oct 2006, pp. 22-29.

[9]. L. Wehenkel and M. Pavella, "Preventive vs. Emergency Control of Power Systems," IEEE Power Energy Society Power Systems Conf. & Exposition, Vol. 3, 2004, pp. 1665 - 1670.

[10]. D. Ernst, L. Wehenkel and M. Pavella, "What is The Likely Future of Real-Time Transient Stability," IEEE Power Energy Society Power Systems Conf. and Exposition, 2009, pp. 1 - 3 .

[11]. A. Hoballah, and István Erlich," Transient Stability Assessment Using ANN Considering Power System Topology Changes," IEEE 15th International Conference on Intelligent System Applications to Power Systems, 2009, pp. 1.

[12]. N.G. Hingorani, L. Gyugyi, "Understanding FACTS: Concepts and Technology of Flexible AC Transmission Systems", Wiley-IEEE Press, New York, 2000.

[13]. A. Edris, "FACTS technology development: an update," IEEE Eng. Review, Vol. 20 2000, pp.4-9.

[14]. R.Mohan Marthur and Rajiv K.Varma "Thyristor Based-FACTS Controllers for Electrical Transmission Systems",IEEE Computer Society Press, 2002.

[15]. L. Kirschner, D. Retzmann. and G. Thumm "Benefits of FACTS for Power System Enhancement," Transmission and Distribution Conference and Exhibition Asia and Pacific, 2005 IEEE/PES, pp.1 – 7.

[16]. Y. Ou; C. Singh, "Improvement of Total Transfer Capability Using TCSC and SVC," Power Engineering Society Summer Meeting, 2001. IEEE , Vol. 2, July 2001, pp. 944-948.

[17]. X. Yu, C. Singh, S. Jakovljevic, D. Ristanovic and G. Huang, " Total Transfer Capability Considering FACTS and Security Constraints," Transmission and Distribution Conference and Exposition, Vol. 1, Sept. 2003, pp.73 - 78.

[18]. C. W. Taylor, "Improving Grid Behavior", IEEE Spectrum, Vol. 36, No. 6, pp. 40-45, June 1999.

[19]. T. Luor, Y. Hsu, T. Guo, J. Lin, and C. Huang, "Application of Thyristor-Controlled Series Compensators to Enhance Oscillatory Stability and Transmission Capability of Longitudinal Power System", IEEE Transactions on Power System, Vol. 14, No. 1, pp. 179-185, Feb. 1999.

[20]. Canadian Electrical Association, "Static Compensators for Reactive Power Control," Context Publications, 1984.

[21]. Nabavi-Niaki, A., Iravani, M.R., 1996, 'Steady-state and Dynamic Models of Unified Power Flow Controller (UPFC) for Power System Studies', IEEE Trans. Power Systems 11(4) 1937–1943.

[22]. Fuerte-Esquivel, C.R., Acha, E., Ambriz-Pe´rez, H., 2000b, 'A Comprehensive UPFC Model for the Quadratic Load Flow Solution of Power Networks', IEEE Trans. Power Systems 15(1) 102–109.

[23]. E. Asha, C. R. Fuerte Esquival, H. ambriz, and C. A. Camacho, "Modeling and Simulation in Power Networks" John Wiley & Sons Ltd, The Atrium, Southern Gate, Chichester, 2004.

[24]. B. R. Gupta, "Power System Analyssis and Design", S. Chand & company LTD. India,1998

[25]. K. Venkateswarlu, Ch. S. Babu and K.K. Kuthadi "Improvement of Voltage Stability and Reduce Power Losses by Optimal Placement of UPFC device by using GA and PSO", International Journal of Engineering Sciences Research-IJESR, Vol 01, Issue 02, May, 2011.